

AO-A103 004

OXYGEN EVOLUTION KINETICS AT POROUS NICKEL ELECTRODES  
(U) AEROSPACE CORP EL SEGUNDO CA CHEMISTRY AND PHYSICS  
LAB A H ZIMMERMAN ET AL. 03 AUG 87 TR-0006(6943)-4

1/1

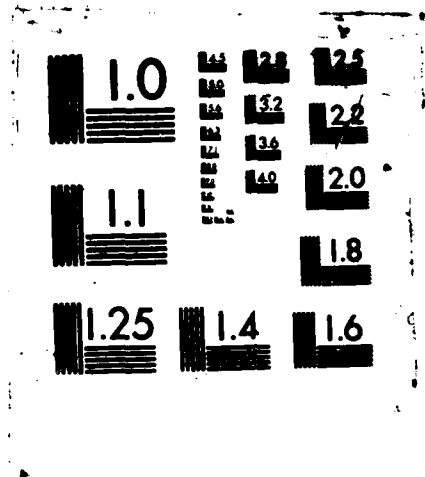
UNCLASSIFIED

SD-TR-87-44 F04701-85-C-0006

F/G 3/1

NL

|  |  |  |  |  |  |  |  |  |  |  |  |  |                    |
|--|--|--|--|--|--|--|--|--|--|--|--|--|--------------------|
|  |  |  |  |  |  |  |  |  |  |  |  |  |                    |
|  |  |  |  |  |  |  |  |  |  |  |  |  | END<br>4 81<br>BLC |



MICROCOPY RESOLUTION TEST CHART  
NATIONAL BUREAU OF STANDARDS-1963-A

AD-A183 884

DTIC FILE COPY

(12)

## Oxygen Evolution Kinetics at Porous Nickel Electrodes

A. H. ZIMMERMAN and P. K. EFFA  
Chemistry and Physics Laboratory  
Laboratory Operations  
The Aerospace Corporation  
El Segundo, CA 90245

3 August 1987

DTIC  
ELECTE  
AUG 25 1987  
S D  
C&D

Prepared for  
SPACE DIVISION  
AIR FORCE SYSTEMS COMMAND  
Los Angeles Air Force Station  
P.O. Box 92960, Worldway Postal Center  
Los Angeles, CA 90009-2960

APPROVED FOR PUBLIC RELEASE;  
DISTRIBUTION UNLIMITED

*A12-183 554*

**REPORT DOCUMENTATION PAGE**

|   |       |  |   |  |                    |                         |
|---|-------|--|---|--|--------------------|-------------------------|
| 1a. REPORT SECURITY CLASSIFICATION<br>Unclassified  |       |  | 1b. RESTRICTIVE MARKINGS  |  |                    |                         |
| 2a. SECURITY CLASSIFICATION AUTHORITY   |       |  | 3. DISTRIBUTION / AVAILABILITY OF REPORT<br>Approved for public release;<br>distribution unlimited  |  |                    |                         |
| 2b. DECLASSIFICATION / DOWNGRADING SCHEDULE   |       |  |   |  |                    |                         |
| 4. PERFORMING ORGANIZATION REPORT NUMBER(S)<br>TR-0086(6945)-4  |       |  | 5. MONITORING ORGANIZATION REPORT NUMBER(S)<br>SD-TR-87-44  |  |                    |                         |
| 6a. NAME OF PERFORMING ORGANIZATION<br>The Aerospace Corporation<br>Laboratory Operations   |       | 6b. OFFICE SYMBOL<br>(if applicable)     | 7a. NAME OF MONITORING ORGANIZATION<br>Space Division   |  |                    |                         |
| 6c. ADDRESS (City, State, and ZIP Code)<br>El Segundo, CA 90245   |       |  | 7b. ADDRESS (City, State, and ZIP Code)<br>Los Angeles, CA 90009-2960   |  |                    |                         |
| 8a. NAME OF FUNDING / SPONSORING ORGANIZATION   |       | 8b. OFFICE SYMBOL<br>(if applicable)     | 9. PROCUREMENT INSTRUMENT IDENTIFICATION NUMBER<br>F04701-C-85-0086-P00016<br><i>-8</i>   |  |                    |                         |
| 8c. ADDRESS (City, State, and ZIP Code)   |       |  | 10. SOURCE OF FUNDING NUMBERS   |  |                    |                         |
|   |       |  | PROGRAM ELEMENT NO.   | PROJECT NO.  | TASK NO.           | WORK UNIT ACCESSION NO. |
| 11. TITLE (Include Security Classification)<br>Oxygen Evolution Kinetics at Porous Nickel Electrodes  |       |  |   |  |                    |                         |
| 12. PERSONAL AUTHOR(S)<br>Zimmerman, Albert H. and Effa, Peter K.   |       |  |   |  |                    |                         |
| 13a. TYPE OF REPORT   |       | 13b. TIME COVERED<br>FROM _____ TO _____ |   | 14. DATE OF REPORT (Year, Month, Day)<br>3 August 1987 |                    | 15. PAGE COUNT          |
| 16. SUPPLEMENTARY NOTATION  |       |  |   |  |                    |                         |
| 17. COSATI CODES  |       |  | 18. SUBJECT TERMS (Continue on reverse if necessary and identify by block number)<br>Nickel electrodes , Sintered electrodes<br>Nickel hydroxides ,<br>Tafel slopes , |  |                    |                         |
| FIELD   | GROUP | SUB-GROUP                                |   |  |                    |                         |
|   |       |  |   |  |                    |                         |
| 19. ABSTRACT (Continue on reverse if necessary and identify by block number)<br><br>The impedance of porous nickel electrodes has been measured under conditions of steady-state oxygen evolution. Significant effects are observed due to the pore structure of the electrodes, and these effects are found to correlate with loading levels, performance, and composition. The oxygen evolution characteristics of sintered plate electrodes have been investigated as a convenient means for determining the structural uniformity and the overall quality of such plates for use as battery electrodes.<br><br><i>Keywords: _____</i> |       |  |   |  |                    |                         |
| 20. DISTRIBUTION / AVAILABILITY OF ABSTRACT<br><input type="checkbox"/> UNCLASSIFIED/UNLIMITED <input checked="" type="checkbox"/> SAME AS RPT <input type="checkbox"/> DTIC USERS  |       |  |   | 21. ABSTRACT SECURITY CLASSIFICATION<br>Unclassified   |                    |                         |
| 22a. NAME OF RESPONSIBLE INDIVIDUAL   |       |  | 22b. TELEPHONE (Include Area Code)  |  | 22c. OFFICE SYMBOL |                         |

CONTENTS

I. INTRODUCTION..... 3

II. EXPERIMENTAL RESULTS..... 5

III. RESULTS AND DISCUSSION..... 9

IV. SUMMARY..... 23

REFERENCES..... 25



|                      |                                     |
|----------------------|-------------------------------------|
| Accession For        |                                     |
| NTIS CRA&I           | <input checked="" type="checkbox"/> |
| DTIC TAB             | <input type="checkbox"/>            |
| Unannounced          | <input type="checkbox"/>            |
| Justification .....  |                                     |
| By .....             |                                     |
| Distribution / ..... |                                     |
| Availability Codes   |                                     |
| Dist                 | Avail and/or Special                |
| A-1                  |                                     |

## FIGURES

|    |   |    |
|----|---|----|
| 1. | Experimental Apparatus Used for Electrode Cycling, Monitoring, and Impedance Measurements.....  | 7  |
| 2. | Voltage Response of a Nickel Electrode to a 20% Increase in Current While in Overcharge at Various Rates.....                           | 10 |
| 3. | Typical Tafel Plots for Nickel Electrodes During Steady State Overcharge.....   | 11 |
| 4. | The Dependence of Current Density at 0.45 Volts (vs.Hg/HgO) on Loading Level During Low Rate Nickel Electrode Overcharge.....           | 13 |
| 5. | Plots of the Logarithm of the Resistance as a Function of Voltage for Three Electrodes with Differing Loading Levels.....               | 15 |
| 6. | Resistance as a Function of Voltage for Nickel Electrodes with a Loading of 0.13 g of Active Material in 1 cm <sup>2</sup> Samples..... | 17 |
| 7. | Effects of High Rate Cycling on Resistance as a Function of Voltage for a Nickel Electrode.....   | 19 |
| 8. | Variation in $\Delta \log R$ as a Function of Tafel Slope for Nickel Electrodes.....  | 21 |

## I. INTRODUCTION

Under conditions of overcharge, nickel electrodes evolve oxygen from the surface of the charged nickel hydroxides that serve as the active material in the electrodes. The kinetics of the oxygen evolution reaction generally have a significant controlling influence on the recharge and self-discharge characteristics of the nickel electrode during battery cell operation. Numerous kinetic studies of oxygen evolution at both planar and porous nickel electrodes have been carried out and have been reviewed by Milner and Thomas (Ref. 1). Particularly for porous electrodes, a wide range of Tafel slopes have been observed (Ref. 2), and a number of mechanistic variations have been proposed to account for the observed range of behavior.

The kinetics of oxygen evolution at porous nickel electrodes are often complicated both by concentration polarization within the porous matrix and by variations in active surface area with rate due to surface shielding by bubble coverage. Milner and Thomas (Ref. 1) present data indicating that concentration polarization and shielding effects can begin to be important at rates as low as  $C/20$  ( $0.5 \text{ ma/cm}^2$ ) for sintered nickel electrodes. The purpose of the work presented here is to use kinetic data obtained from impedance measurements during the charging process to study the mechanisms for oxidation processes in the nickel electrode, and specifically to evaluate how kinetic data can be used to indicate active nickel electrode surface area as well as to what extent the porous structure of sintered electrodes influence the Tafel slopes typically observed at current densities used in battery cells. The changes in porous structure that result from precipitation of nickel hydroxide active material in the sintered plate, as well as changes that occur during cycling of plates are of particular interest. The electrochemical kinetics of oxygen evolution from sintered plate electrodes has been explored in this work as a convenient means of determining the structural uniformity and the overall quality of sintered plates for use as battery electrodes.

## II. EXPERIMENTAL RESULTS

Nickel test electrodes were made by electrochemically depositing nickel hydroxide in sintered nickel plate by cathodic polarization. The electrodes were 1 cm square in all cases, giving a superficial electrode area of 2 cm<sup>2</sup>. The nickel sinter had a porosity of about 80%. Electrochemical deposition was done by cathodic polarization of the sinter in a refluxing (about 85 deg C) solution containing 60% by volume aqueous 2M nickel nitrate and 40% by volume ethanol. Additives such as cobalt hydroxide, manganese hydroxide, or zinc hydroxide were incorporated into the active material of some electrodes by substituting the appropriate 2M aqueous metal nitrate solution for 5% of the nickel nitrate solution. The amount of active material deposited in each electrode (loading level) depended on the time and rate of deposition, with lower rates and longer times giving the higher loading levels. Systematic variations in loading level were typically produced by varying deposition time using a constant deposition rate. The range of loading levels achieved was from about 0.2 to 2.4 g/cc of void volume. The higher loading levels could only be readily achieved by using deposition rates of 20 ma/cm<sup>2</sup> or lower.

All electrodes were electrochemically cycled in a closed plastic cell, which was filled with KOH electrolyte (31% by weight). The cell was equipped with gold-plated feed throughs to which the working, counter, and reference electrodes were connected by nickel clips and nickel wires. The counterelectrode was a 1 inch square nickel metal sheet. A Hg/HgO reference electrode was employed for all voltage measurements, and all voltages reported are corrected for the IR drop between the working electrode and the reference electrode. This IR drop was obtained from the short time (1 msec) voltage response to a small amplitude current change, and typically corresponded to a resistance of 0.3 to 0.5 ohms. The test cell was continuously purged with slowly flowing nitrogen to prevent contamination by atmospheric carbon dioxide. All electrodes were operated at ambient temperature, which was 22±2 deg C.

The experimental apparatus used to control the electrode cycling and to measure kinetic characteristics is indicated in Fig. 1. The electrode was operated in a constant current mode, where the current was provided by a high speed (20 microsecond response time) bipolar power supply (Kepco BOP-36-5M). The power supply current was controlled at a summing junction by two control voltages generated by a microprocessor; one voltage providing a 50 ma range of current and the other voltage providing an additional 2.5 ma of current for a full scale signal. The low current control signal allowed very small amplitude changes in the operating current to be accurately controlled by the microprocessor. The current passing through the working electrode was monitored by measuring the voltage drop across a resistor using a high impedance differential buffer amplifier having a gain of unity. The voltage between the working electrode and the reference electrode was likewise monitored by the microprocessor through a high impedance differential buffer amplifier. The microprocessor also generated an offset voltage that was subtracted from the working electrode voltage, and the difference multiplied by either 500 or 1000 was monitored by the microprocessor as a function of time. The time resolution for monitoring the voltage was 1 msec. The offset amplifier allowed the microprocessor to accurately monitor millivolt level changes in electrode voltage as a function of time. These voltage transient functions were stored by the microprocessor on disk along with data on electrode voltage and current during charge and discharge operation. The microprocessor was also interfaced to an x-y plotter, allowing all stored data files to be processed and plotted as desired.

Impedance measurements were done for nickel electrodes by applying a current step to the electrode while it is charging at a constant rate. The amplitude of the applied current step was chosen by the microprocessor to give a voltage change for the electrode of about 3-5 mv, a change sufficient to be accurately monitored by the microprocessor. The microprocessor monitored the voltage response as a function of time until a steady state condition was reached. The impedance was determined as a function of time from the ratio of the voltage response to the current step, or as a function of frequency from the ratio of the Laplace transforms of the voltage response and the current



step (Ref. 3). Electrode resistance  $R$  is defined as the low frequency limit of the impedance and is given by the change in steady state voltage in response to the current step divided by the current step.

### III. RESULTS AND DISCUSSION

Typical voltage transient responses obtained from nickel electrodes during steady-state overcharge are indicated in Fig. 2 for a range of overcharge rates. The electrodes were charged at a C/5 rate for 9 hr before the transient measurements were made, insuring that the electrode was in a steady-state oxygen evolution condition. The changes in the shapes of the transients, indicated in Fig. 2 as the overcharge current is changed are noteworthy. At an overcharge current of  $1 \text{ ma/cm}^2$ , the response follows an exponential time response quite closely, although this shows up as an "S" shaped curve on the square root of time axis used in Fig. 2. The exponential time response indicates that the overcharge reaction kinetics are controlled by an activation controlled electrochemical process at this low current density, rather than by concentration polarization or bubble shielding effects. As the current density is increased in Fig. 2 the voltage response tends to rise more sharply at short times, until eventually at high current densities, on the order of  $9 \text{ ma/cm}^2$ , the voltage response initially rises linearly with the square root of time, after which it levels out into a steady state condition. A voltage that changes linearly with the square root of time in this manner indicates that mass transport processes in the electrode are controlling the polarization characteristics. The leveling off of the voltage transient is due to the time required to establish a steady-state concentration gradient across the thickness of the diffusion layer, which in this case is likely to simply involve the thickness of the porous electrode structure.

The current/voltage relationships that were measured for a number of nickel electrodes are indicated in Fig. 3, where the electrodes have been chosen to cover a range of loading levels. The primary effect of decreasing loading level in Fig. 3 is to offset the current/voltage lines to the right. This effect arises from the decrease in surface area of active material available in the electrode for oxygen evolution as the loading level is decreased. However secondary effects are observed in the data of Fig. 3 as evidenced by the two electrodes shown having similar loading levels, but significantly

# Voltage Response for Ni Electrode in Overcharge at Various Rates

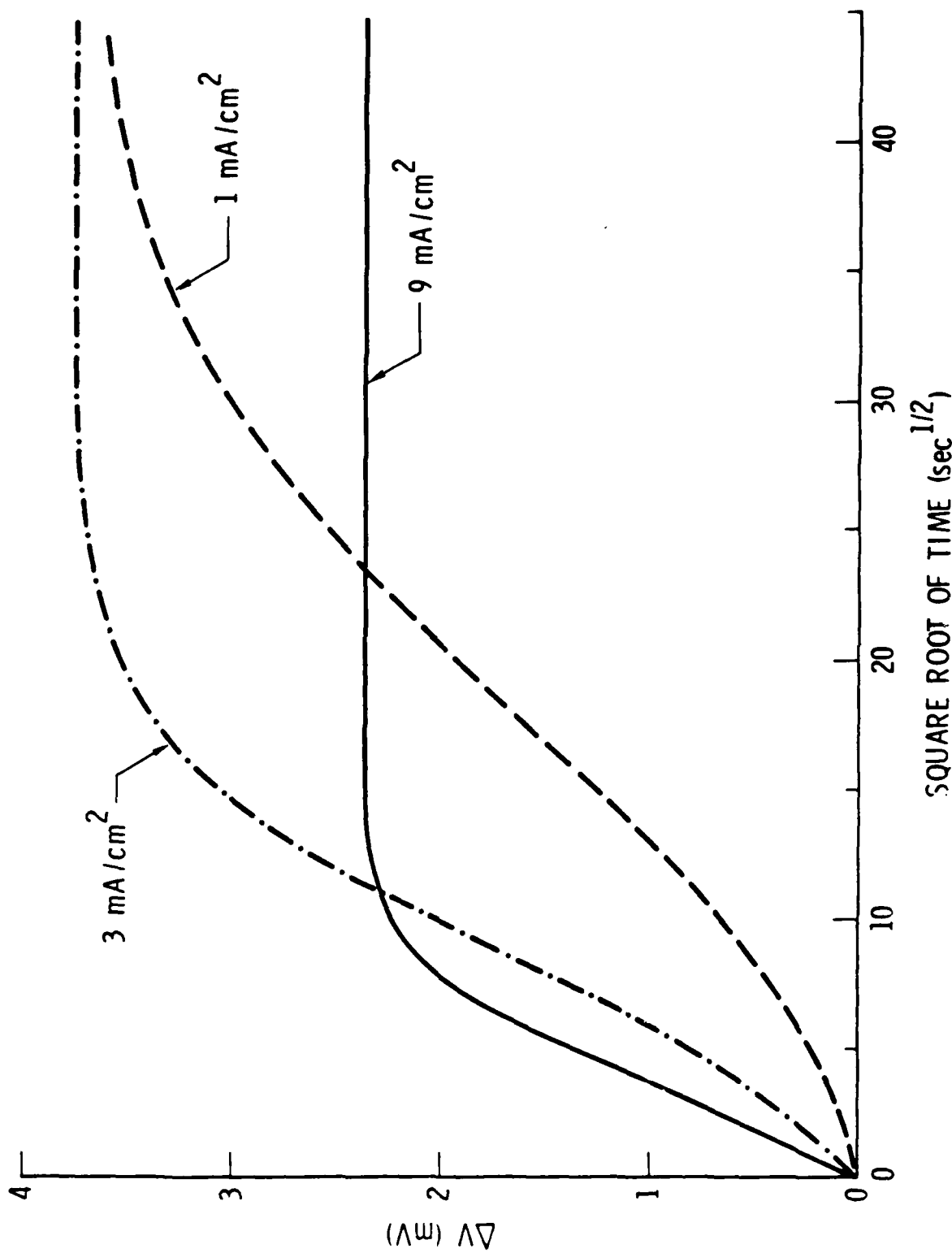


Fig. 2. Voltage Response of a Nickel Electrode to a 20% Increase in Current While in Overcharge at Various Rates.

### Typical Tafel Plots for Ni Electrodes in Overcharge

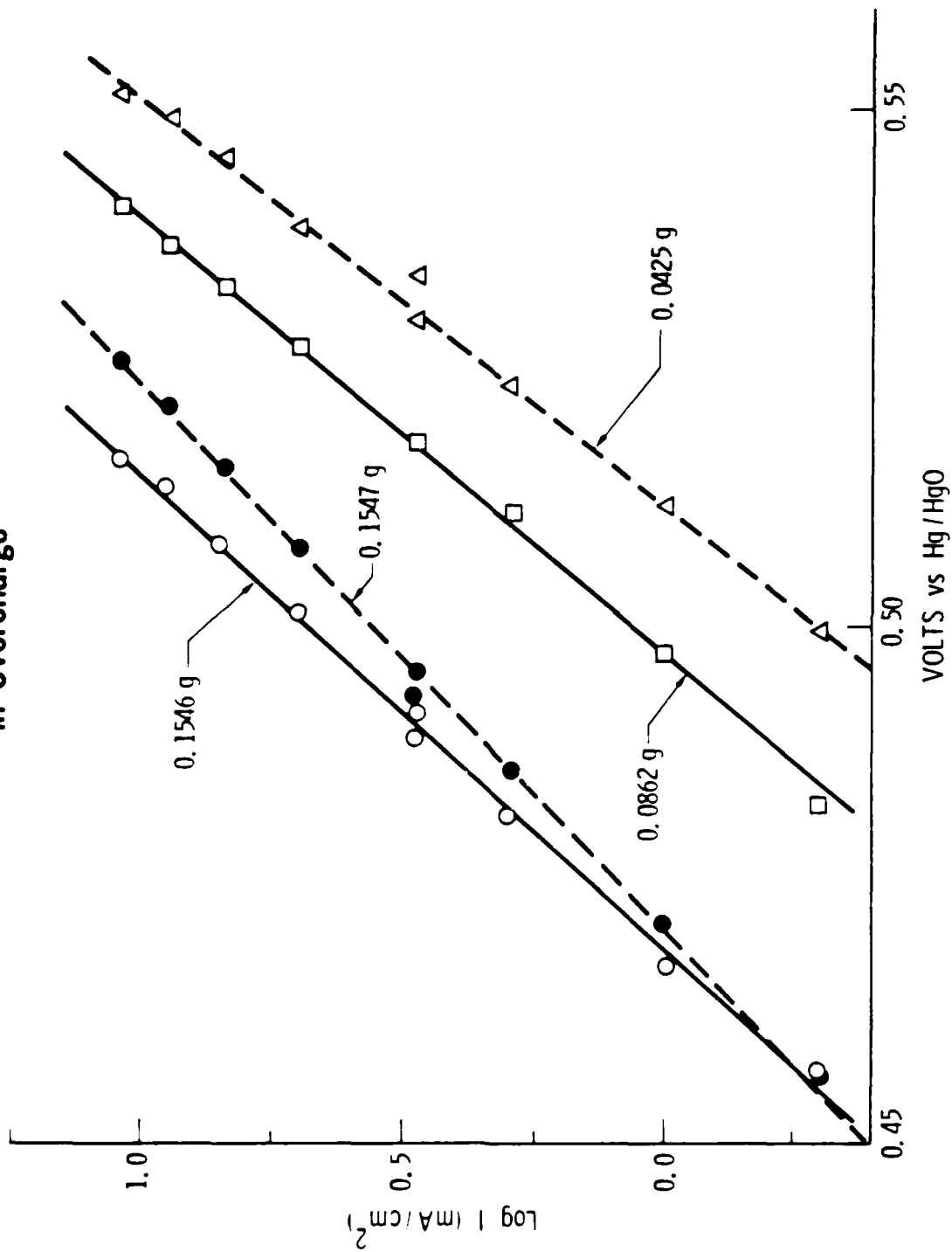


Fig. 3. Typical Tafel Plots for Nickel Electrodes During Steady State Overcharge. The numbers with each line refer to the loading level of that electrode in grams of active material for a  $1 \text{ cm}^2$  electrode.

different slopes (the slope of the logarithm of the current when plotted as a function of the voltage is termed the Tafel slope). If these changes in slope are due to polarization effects in the porous sinter structure, as has been suggested by Milner and Thomas (Ref. 1), then the voltage obtained at the lowest currents where concentration polarization is not expected to be important should give an indication of the relative active material surface area.

The correlation of the current at a relatively low voltage (0.45 V) is indicated in Fig. 4, a correlation which ideally would be expected to be linear if surface area is proportional to the amount of active material in the electrode. The results in Fig. 4 appear to follow two different straight line regions, one for loading levels below about  $0.1 \text{ g/cm}^2$ , and another segment having a greater slope for higher loading levels. Review of the current/voltage data indicates that the change in slope observed in Fig. 4 at about  $0.1 \text{ g/cm}^2$  results from a 20 mv cathodic offset for all current/voltage lines for electrodes having loading levels higher than this value. When the data are corrected for the 20 mv offset, as indicated in Fig. 4, a reasonably good linear correlation is obtained between low rate I/V behavior and loading level. This correlation does provide a means to determine the relative area of the active material surface in nickel electrodes. A likely reason for the voltage offset at the higher loading levels is that these electrodes had a much lower charging current density in terms of electrochemically active surface area, and thus may have an active material surface with a different composition and thus different voltage characteristics. For example, at higher current densities (based on active area) the active material surface is much more likely to be converted to a  $\gamma$ -NiOOH structure, rather than the  $\beta$ -NiOOH structure attained at lower current densities (Ref. 4). These differences arise because the current densities used in the measurements are kept constant based on superficial current density, rather than on electrochemically active surface area.

The differential resistance of an electrode that exhibits a Tafel, or exponential relationship, of current density on voltage may be simply derived as a function of current or voltage by differentiation.

# Dependence of Current Density on Loading Level at Constant Voltage During Low Rate Ni Electrode Overcharge

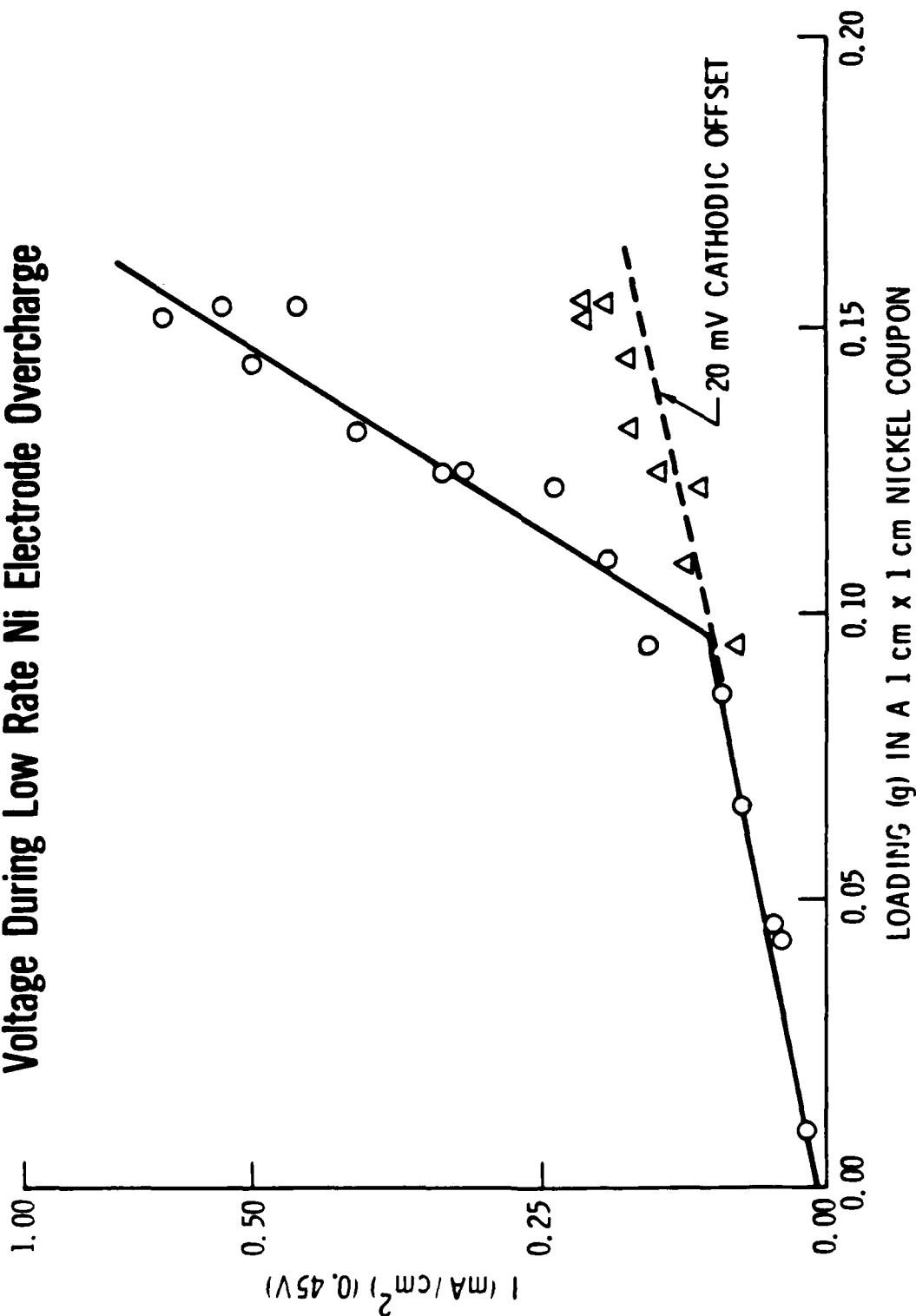


Fig. 4. The Dependence of Current Density at 0.45 volts (vs. Hg/HgO) on Loading Level During Low Rate Nickel Electrode Overcharge. At the high loading levels the dashed line refers to the current calculated by correcting for an apparent 20 mv cathodic voltage offset.

$$I = I_0 \exp(V/b) \quad (1)$$

$$R = dV/dI = b/I = b/(I_0 \exp(V/b)) \quad (2)$$

A plot of the logarithm of the resistance as a function of electrode voltage should therefore be linear, with a slope that is the negative of the Tafel slope.

$$\ln R = -V/b + \ln(b/I_0) \quad (3)$$

Based on Eq. (2), all nickel electrodes operated at a given superficial current density should have the same resistance, independent of the actual active surface area internal to the porous structure. This conclusion results only from the inverse manner in which surface area enters into the resistance relative to the current density, and of course assumes that no change in mechanism is involved that would change the Tafel parameter  $b$ . Thus the constancy of the resistance over a group of electrodes operating at a constant superficial current density provides a very sensitive probe as to whether changes in mechanism are occurring from electrode to electrode.

A plot of  $\log R$  as a function of voltage is indicated in Fig. 5 for three electrodes covering a range of loading levels. Figure 5 clearly illustrates the tendency for the more heavily loaded electrodes to have a greater Tafel slope (units are mv/decade of resistance in Fig. 5, or equivalently mv/decade of current in Fig. 3). The points indicated on each line in Fig. 5 are at a current density of  $12 \text{ ma/cm}^2$ , and the dashed line indicates the resistance obtained at  $12 \text{ ma/cm}^2$  for nickel electrodes with zero loading. The zero loading voltage characteristic was determined by extrapolating the voltage characteristics of the lightly loaded electrodes in Fig. 4 to zero loading. The parameter  $\Delta \log R$  is defined as the difference at a given current density between the resistance measured for a loaded electrode and the resistance measured at the same superficial current density for an electrode with zero loading. This parameter may be thought of as a measure of the increase in the resistance of an electrode due to the fact that the porous structure is

## Effects of Loading Level on Log R vs Voltage Plot

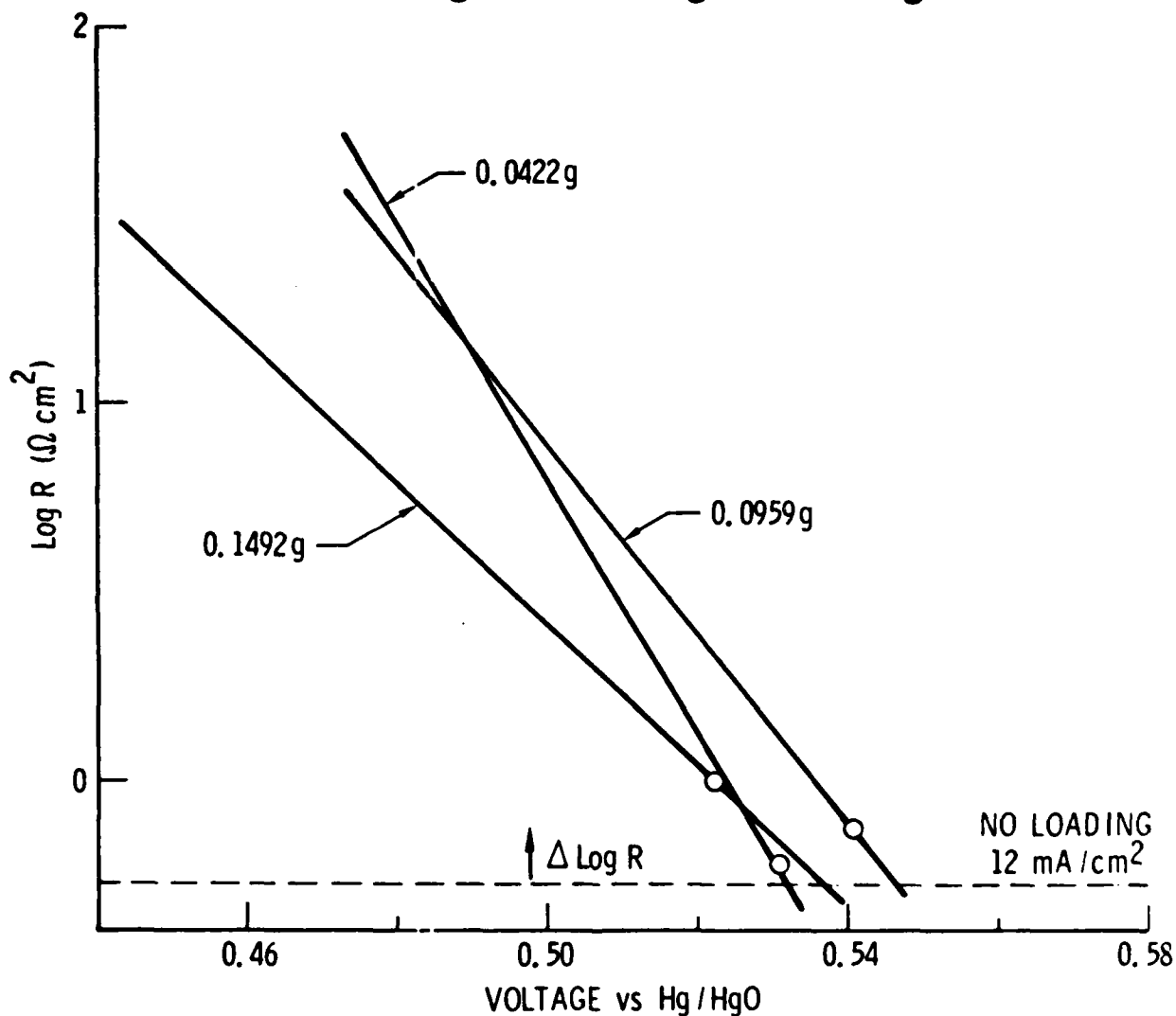


Fig. 5. Plots of the Logarithm of the Resistance as a Function of Voltage for Three Electrodes with Differing Loading Levels. The numbers indicate the loading level for each electrode in g of active material in a 1 cm<sup>2</sup> electrode sample. The points on each line refer to the resistance at a current of 12 ma/cm<sup>2</sup>. The dashed horizontal level is the resistance level for a nickel electrode with zero loading at a current of 12 ma/cm<sup>2</sup>. The  $\Delta \log R$  parameter is indicated as the difference between the dashed level and the point on each line.

partially filled with active material. In this light, the  $\Delta \log R$  parameter should be useful to indicate whether a porous electrode has problems with mass transport through the pore structure or if any blockage of the pores by the active material has taken place. The parameter  $\Delta \log R$  for each of the lines in Fig. 5 at  $12 \text{ ma/cm}^2$  appears to correlate well with the differences in Tafel slopes between these lines.

In Fig. 6 the resistance of four nickel electrodes having a loading level of  $0.13 \text{ g/cm}^2$  has been plotted as a function of voltage. Again the points on these lines indicate the resistance at a current density of  $12 \text{ ma/cm}^2$ , and the dashed line indicates the resistance at  $12 \text{ ma/cm}^2$  for a nickel electrode having zero loading. These data clearly show that although the Tafel slopes may have a dependence on loading level such as was indicated in Fig. 5, the Tafel slopes can vary widely for electrodes having the same loading level. For example, the electrodes in Fig. 6 have Tafel slopes ranging from 40 to 75 mv/decade, while the loading level is the same for all electrodes. However, for the data in Fig. 6 the correlation of  $\Delta \log R$  with Tafel slope is quite good, as was the case for the data presented in Fig. 5. Thus the increase in Tafel slope for some electrodes always appears to accompany increases in the resistance arising from the fact that the porous structure is filled with active material. Such an increased pore resistance may arise from problems with the uniformity of active material in the pore structure. For example, if most of the active material has been deposited near the surface of the pores, much of the internal area and volume of the electrode will be effectively blocked at high rates of operation. This situation would lead to large increases in resistance due to the filling of the porous structure (i.e.,  $\Delta \log R$ ) that would not be observed if the active material were uniformly distributed through the porous structure. Thus the resistance characteristics at relatively high overcharge rates can provide an indication of the uniformity of the active material deposit in the porous structure of sintered electrodes.

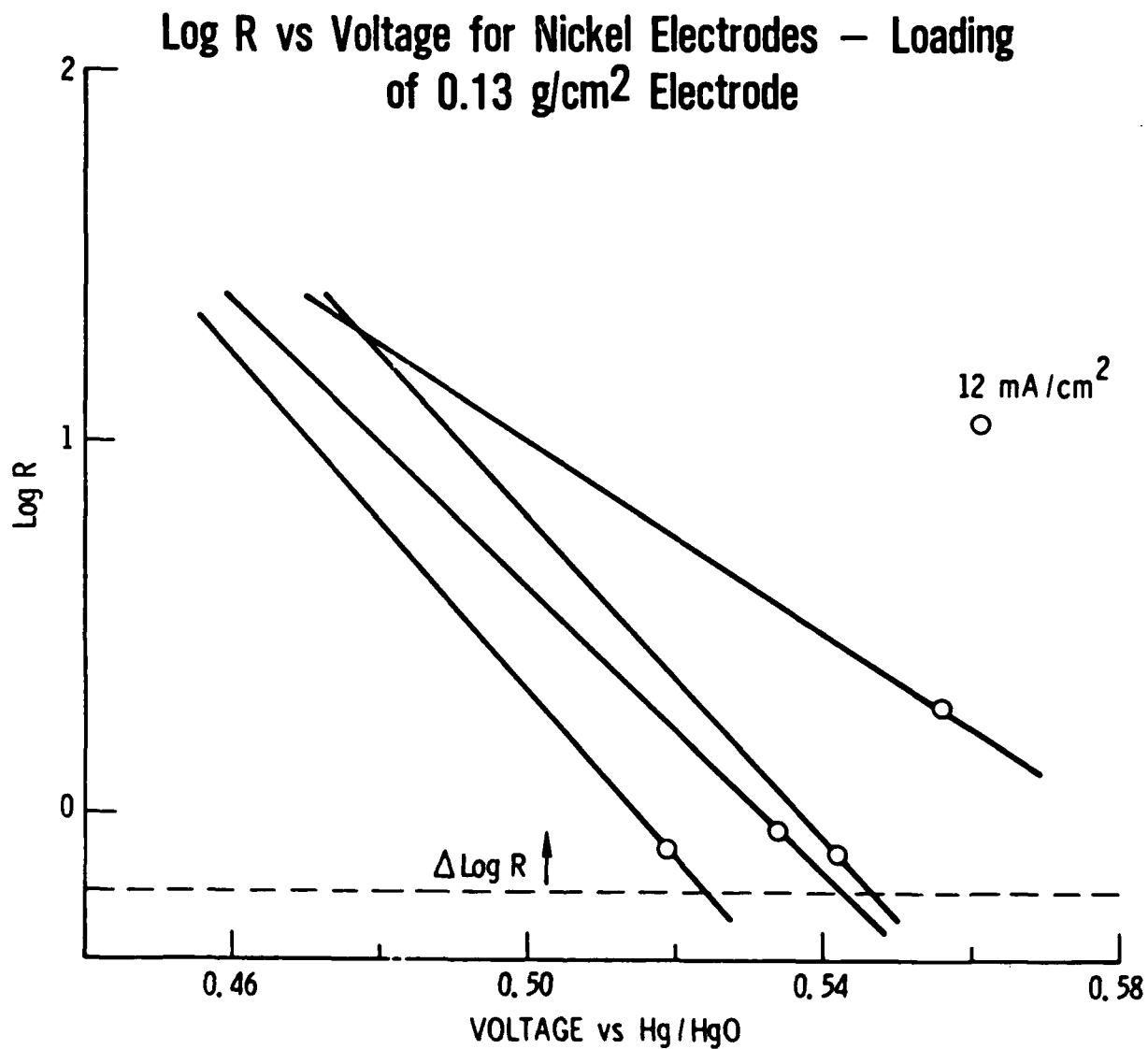


Fig. 6. Resistance as a Function of Voltage for Nickel Electrodes with a Loading of 0.13 g of Active Material in 1 cm<sup>2</sup> Samples. The points on each line, the dashed level, and  $\Delta \log R$  have the same significance as in Fig. 5.

High rate charge/discharge cycling of nickel electrodes, particularly with large amounts of high rate overcharge, are generally recognized as creating significant stresses in the active material deposits internal to the porous electrode. These stresses can cause movement and agglomeration of active material, with the result potentially being a reduction in active material surface area combined with a decrease in how uniformly the active material is distributed in the pore structure. The changes that such cycling cause in the resistance plotted as a function of voltage during overcharge are indicated in Fig. 7. These data were obtained by measuring the resistance characteristics during overcharge for an electrode after about 10 formation cycles, then repeating the resistance measurements after 1000 high rate charge/discharge cycles. The rate used for both charge and discharge during the cycling was the C rate, the depth of discharge was 100%, and the charge return for each cycle was equal to the capacity discharged in the first cycle. During this cycling the electrode capacity increased about 7%. Analysis indicated that little active material was shed from the electrode during the cycling. The resistance characteristics indicated in Fig. 7 show an increase in Tafel slope from 62 to 77 mv/decade resulting from the cycling, along with an anodic voltage offset of about 20 mv. The combination of the voltage offset and the increase in Tafel slope result in a significant increase in resistance,  $\Delta R$  in Fig. 7, particularly at the higher rates of operation. At 12 ma/cm<sup>2</sup> an increase in electrode voltage of about 36 mv was observed as a result of the cycling. In Fig. 7 the voltage offset indicated as  $\Delta V$  at low voltages is likely to be the result of a decrease in the electrochemically active surface area, most likely due to agglomeration of the active material into lumps within the pore structure as a result of the stresses of cycling. The resistance increase indicated as  $\Delta R$  in Fig. 7 (and which corresponds to an increase in  $\Delta \log R$  as defined previously) is likely to be the result of increased blocking of the internal pore structure as the active material moves from being a relatively uniform layer on the walls of the pores to a form that looks more like lumps filling the pores. These physical changes for cycled electrodes relative to uncycled electrodes have been previously characterized by scanning electron microscopy (Ref. 5). The results of Fig. 7 indicate that

# Effects of Cycling on Log R vs Voltage Plot

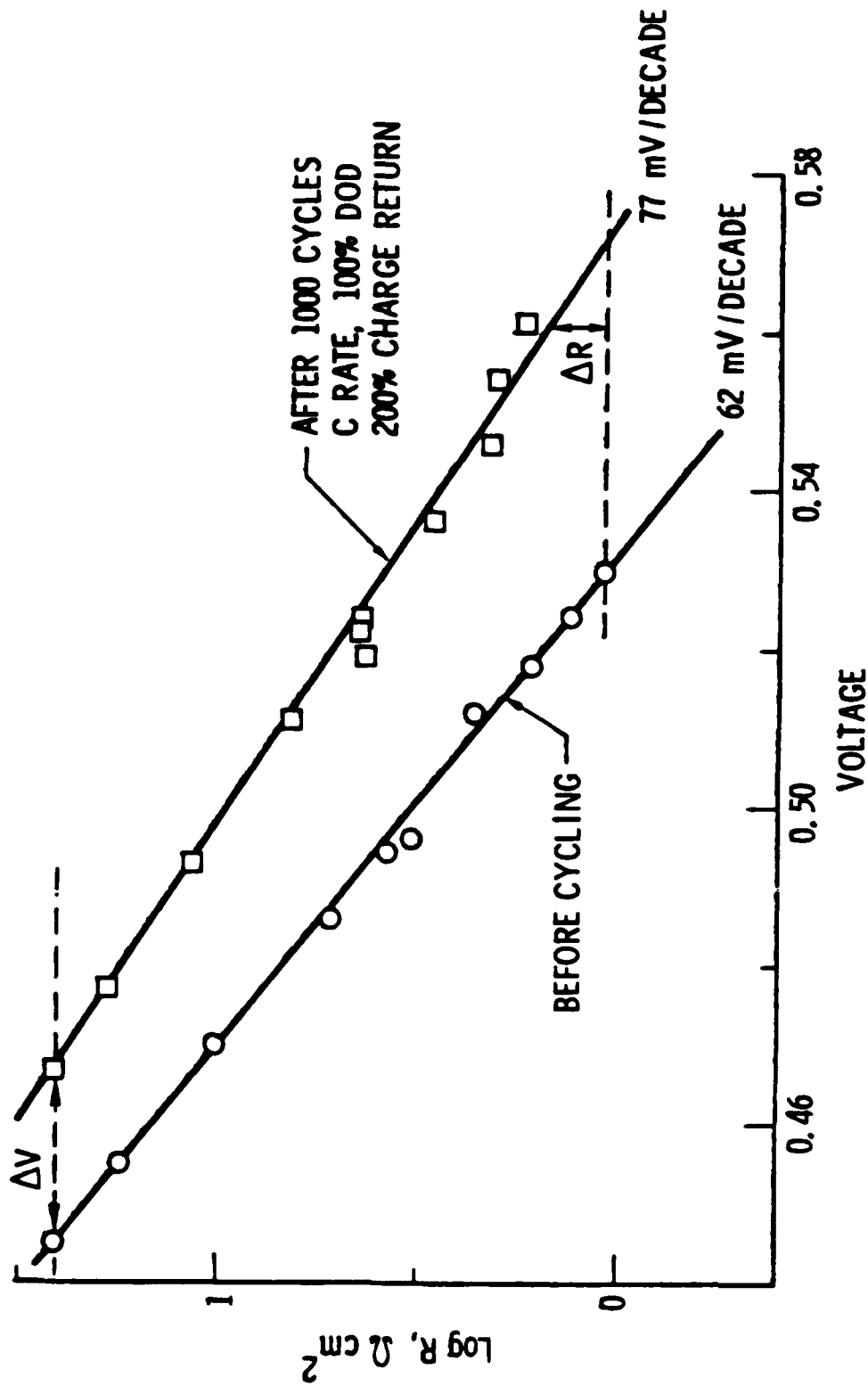


Fig. 7. Effects of High Rate Cycling on Resistance as a Function of Voltage for a Nickel Electrode.

overcharge resistance characteristics can provide a clear indication of the kind of changes that take place in sintered electrodes during their cycle life, even in situations where the net capacity has not yet been degraded by the physical and structural changes.

As indicated in the previous discussions, a correlation was found between the measured Tafel slope and the parameter  $\Delta \log R$ , which gives an indication of the increase in the resistance of a given electrode due to the fact that its pore structure has been loaded with active material. The parameter  $\Delta \log R$  allows a convenient comparison of the I/V slope characteristics for an electrode to a reference I/V slope at a given current density. The reference I/V slope has been chosen to be the nickel electrode with zero loading. As indicated in Eq. (4), the correlation between  $\Delta \log R$  and Tafel slope  $b$  is expected to be proportional to the logarithm of the Tafel slope at constant current.

$$\Delta \log R = \log R - \log R_{\text{ref}} = \log(b/b_{\text{ref}}) - \log(I/I_{\text{ref}}) \quad (4)$$

The correlation is indicated in Fig. 8, where a linear fit to the data has also been indicated. The correlation in Fig. 8 appears to be more linear than logarithmic, suggesting that while superficial current density is held constant, the geometric current density on the active material area is changing with Tafel slope.

The correlation in Fig. 8 has been found to be followed by nickel electrodes of all types and quality that could be obtained or fabricated. The quality of this correlation is somewhat surprising since the electrodes studied include those from a number of commercial battery manufacturers, of both new and failed or degraded vintage, as well as those fabricated in our laboratory both by chemical and electrochemical impregnation. These electrodes contained a variety of special additives in varying concentrations as well as varying widely in loading levels. Electrodes are included in Fig. 8 that cover a wide range of performance characteristics, ranging from very good in terms of utilizing the active material, to electrodes that show less than half of the utilization generally found for new electrodes. It was also noted in this

## Variation in Log R as Function of Tafel Slope for Nickel Electrodes

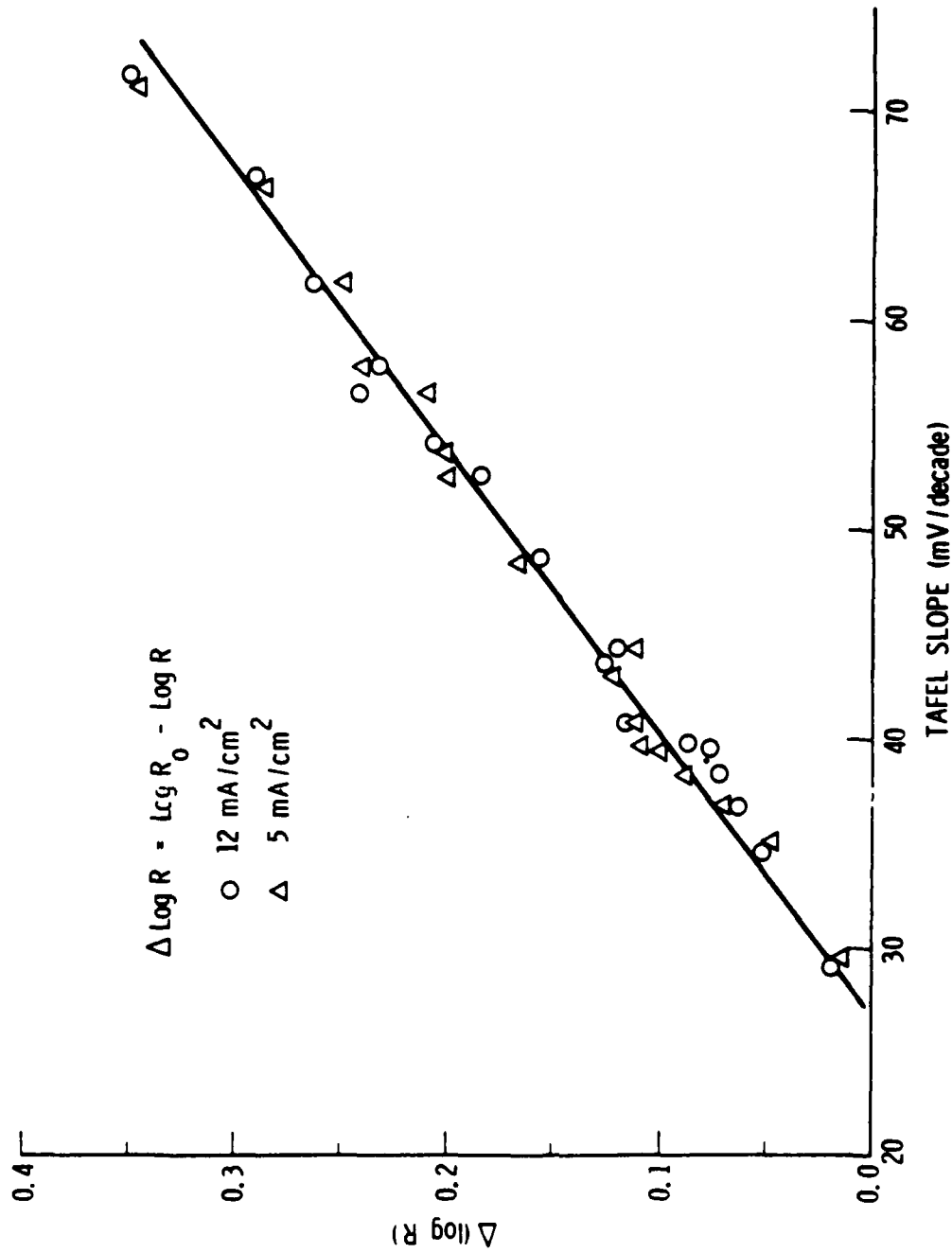


Fig. 8. Variation in  $\Delta \log R$  as a Function of Tafel Slope for Nickel Electrodes.  $\Delta \log R$  is given by the difference indicated in Fig. 5 between the resistance with and that without loading. The circles refer to  $\Delta \log R$  at 12 ma/cm<sup>2</sup>, and the triangles refer to  $\Delta \log R$  at 5 ma/cm<sup>2</sup>.

correlation that new electrodes that showed good utilization of active material generally appeared relatively low on the  $\Delta \log R$  scale, and that these electrodes moved up the correlation line in Fig. 8 as they were cycled and their performance degraded. This trend is clearly indicated by the example shown in Fig. 7. Nickel electrodes that gave good performance over a large number of high rate charge/discharge cycles generally were between 30 and 40 mv/decade on the correlation of Fig. 8 at beginning of life, and moved up the correlation line much more slowly than did electrodes that started their life higher on the correlation line. All electrodes obtained from the various battery manufacturers that were not degraded from their beginning of life characteristics were in the lower region of the correlation of Fig. 8, between 30 and 40 mv/decade.

The correlation indicated in Fig. 8 provides a convenient means of classifying nickel electrodes as to the overall quality of the active material deposit in the sinter. Electrodes that are loaded too heavily or electrodes that are loaded nonuniformly could be very easily screened by either a Tafel slope measurement or by measuring the resistance at a current density of about 12 ma/cm<sup>2</sup>. The resistance measurement is particularly convenient because it is a single point measurement that can be done very rapidly during a test sequence, whereas a Tafel slope measurement is time consuming and is likely to constitute an entire test sequence in itself. This kind of screening would be particularly valuable in evaluating or changing electrode fabrication techniques since it provides rapid feedback, indicating product quality without the necessity for extensive life-test matrices.

#### IV. SUMMARY

The kinetics of oxygen evolution from sintered nickel electrodes has been studied on a wide range of electrodes of varying loading levels and varying performance characteristics. The kinetic behavior at low current densities can provide information on the total active material surface area. At high current densities the effects of pore structure loading can be seen as an increased resistance for oxygen evolution. Resistance increases from the pore loading that are unusually high appear to correlate well with performance changes and capacity losses during extensive charge/discharge cycling.

#### REFERENCES

1. P. C. Milner and U. B. Thomas, "Advances in Electrochemistry and Electrochemical Engineering," Interscience Publishers, New York, 1967, Vol. 5, pp 1-87.
2. B. E. Conway and P. L. Bourgault, "Can, J. Chem." 40,1690(1962).
3. A. A. Pilla, "J. Electrochem. Soc." 117,467(1970).
4. R. Barnard, C. F. Randell, and F. L. Tye, "J. Applied Electrochem." 10,127(1980)
5. A. H. Zimmerman, "J. Power Sources" 12,233(1984).

END

9-87

DTIC